



# Current perspectives in conventional and advanced imaging of the distal radioulnar joint dysfunction: review for the musculoskeletal radiologist

Aishwarya Gulati<sup>1</sup> · Vibhor Wadhwa<sup>2</sup> · Oganesh Ashikyan<sup>3</sup> · Luis Cerezal<sup>4</sup> · Avneesh Chhabra<sup>3,5,6</sup>

Received: 25 December 2017 / Revised: 27 July 2018 / Accepted: 1 August 2018 / Published online: 1 September 2018  
© ISS 2018

## Abstract

Distal radioulnar joint (DRUJ) dysfunction is a common cause of ulnar sided wrist pain. Physical examination yields only subtle clues towards the underlying etiology. Thus, imaging is commonly obtained towards an improved characterization of DRUJ pathology, especially multimodality imaging, which is frequently resorted to arrive at an accurate diagnosis. With increasing use of advanced MRI and CT techniques, DRUJ imaging has become an important part of a musculoskeletal radiologist's practice. This article discusses the normal anatomy and biomechanics of the DRUJ, illustrates common clinical abnormalities, and provides a comprehensive overview of the imaging evaluation with an insight into the role of advanced cross-sectional modalities in this domain.

**Keywords** Distal radioulnar joint · DRUJ · Instability · CT · MRI · Dynamic imaging

## Introduction

The distal radioulnar joint (DRUJ) is the distal articulation between the radius and ulna. It is a major weight-bearing joint at the wrist, which distributes forces across the forearm bones [1]. Acute traumatic instability of the DRUJ is often associated with fractures of the “ring” formed by the two bones of the forearm and is usually easy to recognize on radiographs [2, 3]. However, further advanced imaging may be required in cases that are more challenging to diagnose on conventional radiographs, such as chronic processes like early arthritis, resulting

in cartilage loss and bone erosions, ligament abnormalities, altered kinetics in the setting of instability, and occult fractures, among others [4–6]. Understanding the details of anatomy and mechanics of the DRUJ is an important prerequisite to the systematic image interpretation. This article reviews the normal anatomy and biomechanics of the DRUJ, common clinical abnormalities, and provides a comprehensive overview of the imaging evaluation with an insight into the role of advanced cross-sectional modalities in this domain.

## Anatomy and biomechanics

The DRUJ is a pivot joint composed of the radioulnar articulation and soft tissue structures, the major contributors to stability. Supination and pronation are allowed only through complex interactions of the bony joint and soft tissue stabilizers with the proximal radioulnar joint, radiocapitellar joint, and the interosseous membrane.

The bony constituents are the sigmoid notch—a concave articular surface of the distal radius with a radius of curvature of about 15 mm—and the convex surface of the head of the ulna, which has a radius of curvature of 10 mm [7]. The sigmoid notch may exhibit different shapes, such as flat face, ski slope, C type, and S type. The flat face shape has the greatest propensity towards injuries and instability [8]. Along with the proximal radioulnar joint, DRUJ allows

**Electronic supplementary material** The online version of this article (<https://doi.org/10.1007/s00256-018-3042-1>) contains supplementary material, which is available to authorized users.

✉ Avneesh Chhabra  
avneesh.chhabra@utsouthwestern.edu

- <sup>1</sup> Dr. Gulati Imaging Institute, New Delhi, India
- <sup>2</sup> Radiology, University of Arkansas for Medical Sciences, Little Rock, AR, USA
- <sup>3</sup> Radiology, UT Southwestern Medical Center, Dallas, TX, USA
- <sup>4</sup> Radiology, Diagnóstico Médico Cantabria, Santander, Spain
- <sup>5</sup> Orthopaedic Surgery, UT Southwestern Medical Center, 5323 Harry Hines Blvd, Dallas, TX 75390-9178, USA
- <sup>6</sup> Johns Hopkins University, Baltimore, MD, USA

pronation and supination of the forearm, with the former assisted by the pronator teres and pronator quadratus muscles, and the supination aided by the supinator muscle in extension and biceps brachii in flexion. The greater length of curvature of the sigmoid notch with respect to the ulnar head by about 50% permits a combination of rotation and translation during pronation and supination [9, 10]. The contact area in articulation is maximum in the neutral position (about 40–60%), while it is as low as 10% during extremes of pronation and supination [10]. The radius rotates 150° around the fixed ulnar head and additional rotation of up to 30° occurs at the radiocarpal joint allowing a 180° hand arc [9]. It moves distal and dorsal to the ulna during supination, and proximal and volar during pronation, thus a complex “centroid of rotation” is formed rather than a single center of rotation [5]. While rotation of the radius around the ulna remains the predominant movement, the ulnar head, in addition, translates about 2.8 mm in the volar direction during supination, and about 5.4 mm dorsally during pronation [11]. Without soft tissue support, the joint has little intrinsic stability from the bony articulation, which contributes only towards 20% of stabilization [12].

The triangular fibrocartilaginous complex (TFCC), is the main soft tissue support of the DRUJ (Fig. 1). It consists of the volar and dorsal radioulnar ligaments, the triangular fibrocartilage proper (TFC or articular disk), meniscal homologue, ulnolunate and lunotriquetral ligaments (LTL), ulnar collateral ligament, and the extensor carpi ulnaris (ECU) subsheath reinforced medially by the linea jugata [13, 14].

The TFC originates at the junction of the lunate fossa and the sigmoid notch of the radius and inserts at the base and tip of the ulnar styloid process. Along with stabilization, it also facilitates load dispersion and absorption, and allows the six degrees of freedom at the wrist—flexion-extension, supination-pronation, and radial and ulnar deviation [15]. The central cartilaginous weight-bearing area is avascular, but the peripheral margins are thick and well vascularized, forming the dorsal and volar radioulnar ligaments, the primary stabilizers of the DRUJ, which attach directly onto bone at the radius, and not cartilage [7]. Peripheral TFC has a superficial portion (distal lamina), and a deep portion (proximal lamina), which are separated by fibrovascular tissue called ligamentum subcruentum. The distal lamina inserts onto the tip of the ulnar styloid, and the deep inserts at the fovea of the ulnar styloid base in the form of a conjoined tendon along with the ulnocapitate ligament. There is thus increased risk of instability in case of ulnar styloid fracture or fracture of the dorsoulnar corner of the distal radius [16, 17]. As per Hagert, the superficial dorsal and deep volar fibers are tense during pronation and the superficial volar and deep dorsal fibers are tense during supination [18]. The

ulnolunate and ulnotriquetral ligaments connect the ulna to the carpals through the foveal origin of the RU ligament. The meniscal homologue (MH) extends from the tip and lateral aspect of the ulnar styloid to the triquetrum. It is largely composed of fibrous and vascular areolar tissues and creates a continuous arc from the TFC over the ulnar side. The pre-styloid recess is a synovial cavity communicating with the ulnocarpal space that is formed by the fibers of the TFC and MH that attach to the styloid process. The ulnar collateral ligament is thin and fibrous and blends in with the MH and ECU tendon sheath [19].

Tension of the ECU tendon and pronator quadratus during supination provides more extrinsic stability. The interosseous membrane (IM) contributes to additional stability by preventing subluxation of the distal radius. Along with maintaining forearm and DRUJ stability, it also plays an important role in the transmission of load from the wrist to the elbow, and between the forearm bones [20]. A fall on the outstretched hand (FOOSH) can rarely lead to an Essex–Lopresti injury consisting of radial head fracture, rupture of the central band of the interosseous membrane (IM), the interosseous ligament, and DRUJ dislocation/subluxation [21]. The capsule prevents anteroposterior subluxation during pronation and supination [5].

## Clinical features

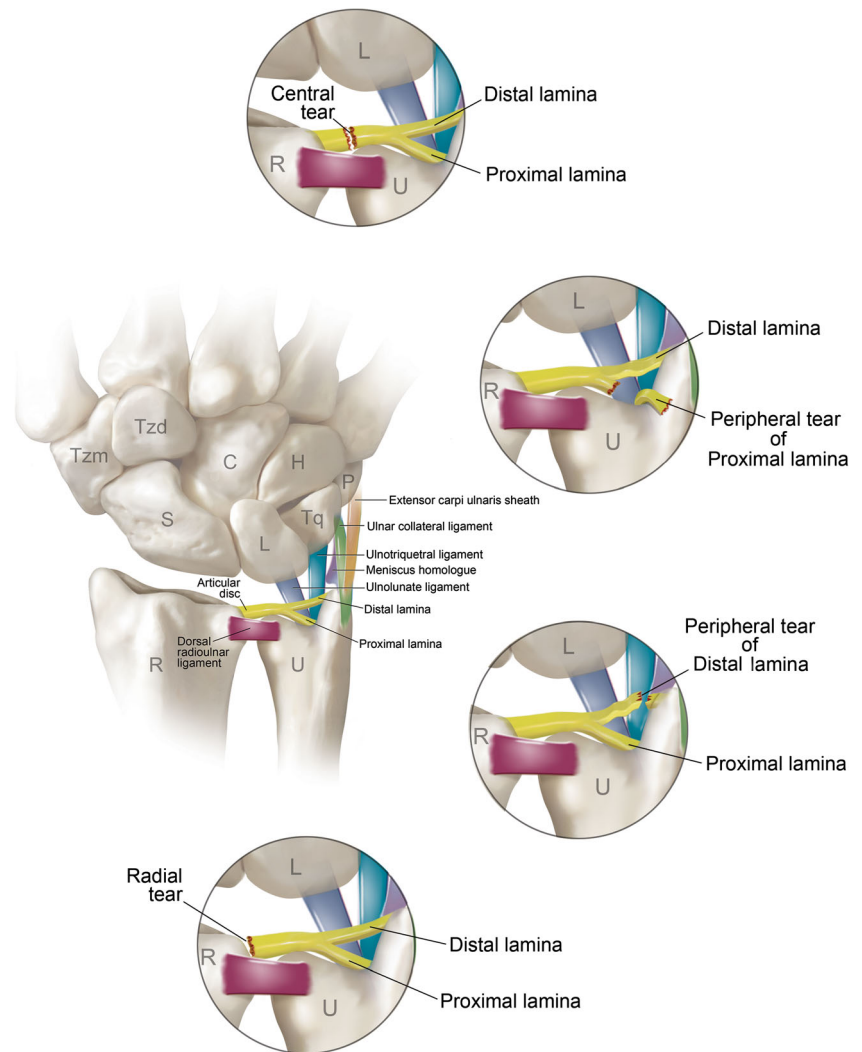
Disorders of the DRUJ can broadly be classified as impaction, incongruity, inflammation and instability [7]. Etiologies of DRUJ dysfunction and/or pain include primary or secondary osteoarthritis, congenital, degenerative, traumatic, infection, inflammatory and ligamentous laxity, among others [22]. Fracture of the distal radius is the most common cause of DRUJ instability in all age groups [23]. In younger patients, Salter Harris Type II fractures have been associated with instability [24]. Secondary instability may be caused by malunion of fractures or growth arrest in younger populations [24]. Isolated TFCC injury without associated fractures can also lead to instability.

Common presentations of DRUJ dysfunction include ulnar sided wrist pain, painful or limited movements, audible snapping or crepitus at the wrist and decreased grip strength or weakness. The patients may also present with obvious physical deformity, redness, and swelling [14, 25]. During a physical examination, it is important to compare the affected and unaffected sides, perform a motor, sensory and vascular assessment of the limb, and test for instability. [5].

There are various clinical tests used specifically to evaluate the DRUJ [5].

The Press Test is an indicator of TFCC dysfunction or tear and has been shown to have 100% sensitivity to

**Fig. 1** Schematic of the anatomy of the major ligaments of the DRUJ and their common pathologies



TFCC abnormality, however, not all TFCC tears manifest as DRUJ instability due to the intact DRUJ ligaments [5, 26]. The Clunk Test assesses the interosseous membrane [5]. For evaluating ECU, the ice-cream test has also been recently proposed [27]. The Stress Test or Ballotement Maneuver (Piano Sign) assesses static instability and has a sensitivity of 66% and specificity of 68% for the evaluation of the palmar and dorsal radioulnar ligaments [5].

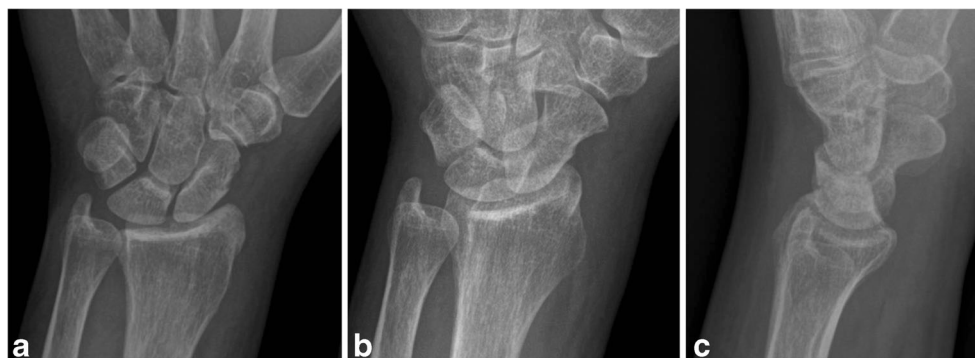
## Radiological evaluation

### Plain radiography

Radiography is the mainstay for the initial evaluation of DRUJ. A three-view wrist series, with posteroanterior (PA), oblique, and lateral projections is typically done (Fig. 2). For a neutral PA radiograph, proper positioning of the forearm is important with the upper arm abducted,

elbow flexed to 90°, and forearm in neutral position with the fingers and thumb in neutral position, forming a flat hand [6]. This view is mainly used for the assessment of degenerative DRUJ and ulnocarpal joint changes, radioulnar space, and ulnar variance. A widened space between the sigmoid notch and the ulna with respect to the unaffected side is a strong indicator of a dorsal ulnar subluxation/dislocation while increased overlap indicates volar ulnar subluxation /dislocation [28]. Dorsal ulnar subluxation is often associated with a fracture of the ulnar styloid process and a shortened radius, along with the widened joint space on the PA views. The lateral view depicts the dislocation clearly. Dislocations of the DRUJ itself are uncommon and may be either dorsal due to hypersupination injuries, which are more common, or volar due to hyperpronation injuries. They are also associated with radial fractures and TFCC injuries. On radiography, the DRUJ space is widened and the ulnar styloid is rotated to the central portion of the ulna (Fig. 3).

**Fig. 2** PA (a), oblique (b), and lateral (c) views of normal DRUJ articulation



Ulnar variance (Hulten variance) or radioulnar index, is a measure of the relative lengths of the radius and the ulna. It is the perpendicular distance in millimeters between a line along the medial articular surface of the distal radius extended toward the ulna and the ulnar fovea [4, 29]. If the ulnar surface is distal to the radius, it is considered a positive variance and if the ulna lies proximal to the radial surface, it is denoted as a negative ulnar variance. This index varies amongst individuals, over an individual's lifetime and with changes in forearm position, and is best measured on the standard PA views [4]. The mean value is 0.9 mm with a range of 2.3 to 4.2 mm [30]. Pathological changes in the ulnar variance alter the distribution of forces across the wrist [29]. A 2.5-mm increase in ulnar variance increases predisposition to ulnar impaction syndrome, also known as ulnar loading or abutment, due to the increased ulnar loading stress between the ulna and carpal bones leading to TFCC tears and disc degeneration, however, this syndrome may also be seen with neutral or negative variance, which may be related to the dynamic impingement (Fig. 4) [6]. A negative ulnar variance has been shown to be associated with ulnar impingement syndrome and Kienböck disease [4].

The oblique and lateral radiographs are optimal for the congruency and alignment of the DRUJ, respectively.

Proper positioning for the lateral position may prove to be difficult for the patients due to pain and decreased range of motion, but is very important, since rotation of as low as 10° can lead to inaccuracies in the measurements [31]. A true lateral view can be evaluated by assessing the scaphopisocapitate alignment (Fig. 5). The volar cortex of the pisiform should lie between the volar cortices of the capitate, the distal pole of the scaphoid, ideally within the central third of this interval [32]. The ulna normally projects 2 mm dorsal to the radius on a true lateral radiograph. A projection beyond 6 mm indicates instability [33]. Indirect indicators of DRUJ instability include fracture of ulnar styloid base, dorsal tilt of the distal radius by 15° or more, ulnar fovea avulsion, radial shortening by 4 mm, and radial inclination less than 0° [5]. Calcification, joint space narrowing, sclerosis, and cysts are also easily detected on radiography, e.g., in conditions such as calcium pyrophosphate deposition disease.

### Ultrasonography

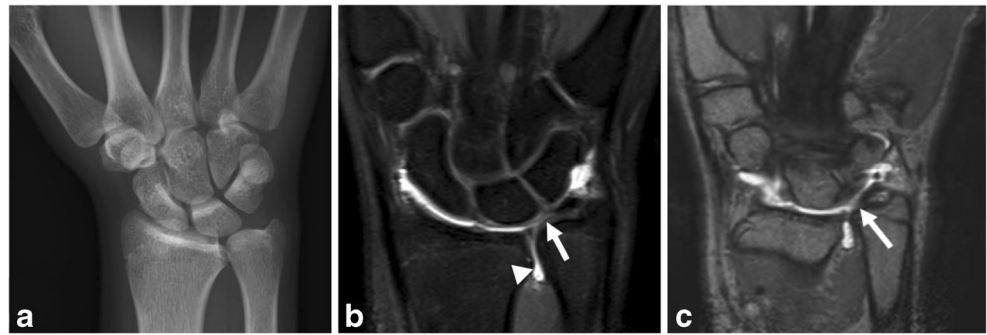
With the frequent use of high frequency and small-size probes, the use of US in musculoskeletal evaluation continues to evolve and expand. Dynamic and real-time evaluation



**Fig. 3** PA (a), oblique (b), and lateral (c) radiographs of the wrist and lateral view of the forearm (d) showing dislocation of the DRUJ and fracture of the distal radius shaft. a, b Widening of distal radioulnar

joint space with positive ulnar variance (*arrow in b*) is consistent with DRUJ dislocation. c Dorsal dislocation of the ulna is seen. d Associated fracture of radial shaft is consistent with Galeazzi fracture-dislocation

**Fig. 4** Ulnocarpal impaction seen on radiograph (a) and MR arthrogram images (b, c). a Ulnolunate abutment with narrowing of the space. b, c Full-thickness central perforation of the TFCC (arrows) with open fluid communication between the DRUJ and ulnocarpal space (arrowhead)



combined with low cost, lack of ionizing radiation risk, and easy availability render US a viable option for soft tissue evaluation. Hess et al. have described a sonographic method of quantifying DRUJ instability by measuring dorsovolar ulnar head translation relative to the distal radius and defining a ratio to differentiate a normal vs. unstable DRUJ [34]. Color Doppler US can also be used to evaluate synovitis in the ulnocarpal recess of the wrist, an indirect sign of TFCC tear. However, US modality use remains limited due to operator dependence, inability to interrogate the ulnocarpal joint, and uncertainty in establishing a final diagnosis.



**Fig. 5** True lateral view of the wrist with normal scaphopisocapitate alignment, i.e., scaphoid position (curved line) between the pisiform and capitate (straight lines)

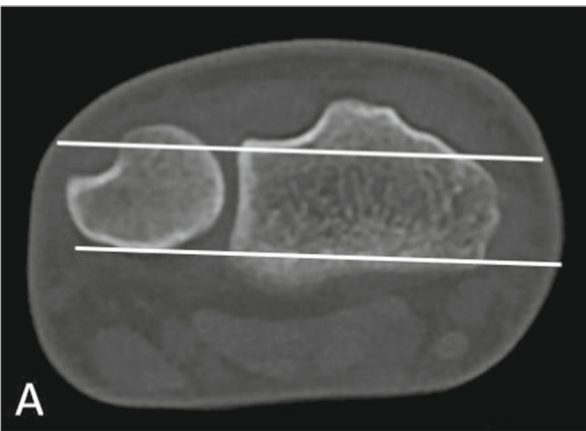
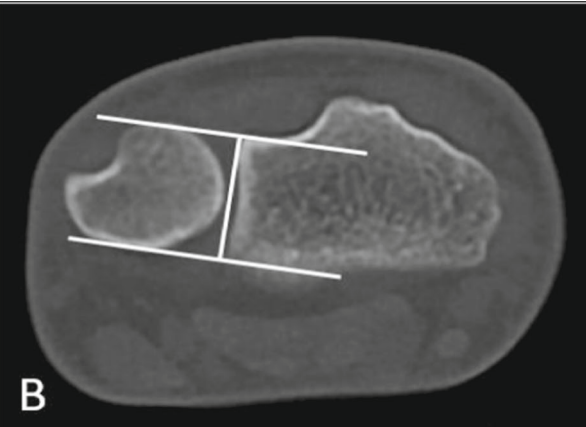
## Computed tomography

CT evaluation of both wrists, to account for normal anatomical variance, remains the gold standard in the evaluation of DRUJ congruency [35]. A static scan acquisition is typically done with the patient supine and the arms overhead in the swimmer or Superman positions in neutral, pronation, and supination positionings. While static CT provides excellent anatomic details, it does not allow real-time dynamic assessment of stress-related changes to the joint. Increasingly, imaging with the joint in neutral position, pronation, and supination with varying loads is being preferred to study the joint motion and the interplay of its soft and bony components. Local anesthetic may be injected to circumvent inaccuracies from restricted range of motion due to patient discomfort as the pain and restricted joint movement may not allow the patient to handle the weights or multi-positional imaging. The loading can be provided either by dead weight application or a special apparatus that provides torque [36]. Three-dimensional renderings of cross-sectional CT images are often created for the referring surgeons for pre-surgical planning.

DRUJ instability is assessed by determining the position of the ulna relative to the radius. Imaging is performed with the field of view extending from immediately above the Lister's tubercle to at least the first row of carpal bones. Axial images are reconstructed parallel to the line joining the radial and ulnar styloid processes depicting the DRUJ articulation. There are various methods to quantify the displacement on these axial images—the radioulnar line (or Mino's) method, the radioulnar ratio method, the subluxation ratio method, epicenter method, and the congruency method (Table 1) [4, 22, 31, 37–40]. The subluxation method and the epicenter method are debated to be the most reliable [37, 41]. The epicenter method takes the normal translation of the DRUJ into account and may be more specific [38].

Kinematic 4D CT is a recent development that allows the assessment of joint kinetics in real time motion with the patient in prone position with the wrists overhead performing a series of movements at the wrist with continuous scanning [42] (Video 1). This modality is

**Table 1** Methods to assess DRUJ instability

Mino's Method		
 <p><b>A</b></p>	<p>Two lines are drawn, one each through the dorsal and volar borders of the radius. These are extended to evaluate the position of the ulna relative to these.</p>	<p>If more than 25% of the ulna lies volar or dorsal to these lines, instability is present</p>
Subluxation Ratio Method and Radioulnar Ratio Method		
 <p><b>B</b></p>	<p>This is a modification of the radioulnar ratio. A line joining the two edges of the sigmoid notch is drawn. Two lines are drawn perpendicular to this line, one passing through the dorsal and one through the volar edge of the sigmoid notch. The maximum extent of the ulna beyond either of these lines is measured and the ratio is compared against the total sigmoid</p>	<p>The mean subluxation ratios in neutral position, pronation and supination are 0.01, 0.20, and -0.13 respectively.</p> <p>The mean radioulnar ratios in neutral position, pronation and supination are 0.51, 0.66, and 0.42 respectively.</p>

technically demanding and requires a high-end scanner with 256- and 320-slice capability to attain the desired temporal resolution of 4–5 images per second and a

coverage area of 10–16 cm (Fig. 6). Iterative reconstruction approach has been suggested to reduce the radiation dose during real-time volume imaging. 3D segmented

**Table 1** (continued)

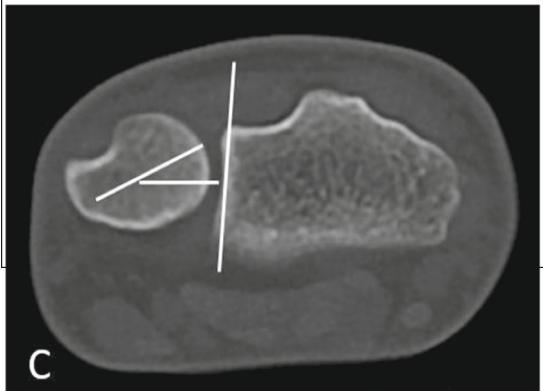
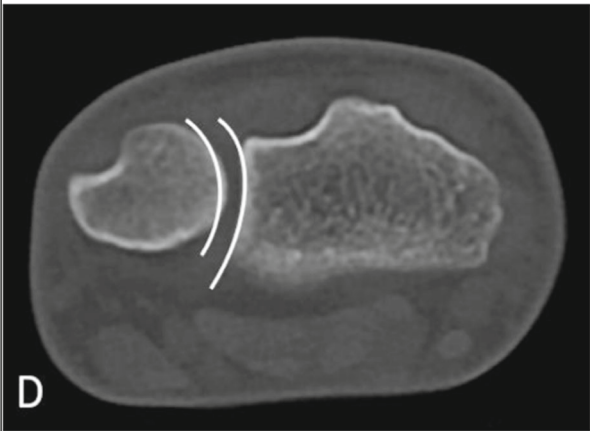
	<p>notch length.</p> <p>For calculating the radioulnar ratio, a line is drawn joining the dorsal and volar edges of the sigmoid notch which depicts the length of the sigmoid notch. A second line is drawn perpendicular to the first that passes through the center of the head of the ulna. The radioulnar ratio is the ratio between the line joining the point of intersection of the two lines with the volar edge of the sigmoid notch and the total length of the sigmoid notch.</p>	
<p>Epicenter Method</p>		
	<p>The centers of the head of the ulna and the styloid process are determined by drawing two circles. The center of rotation of the</p>	<p>If this line is within the middle half of the sigmoid notch, the DRUJ is considered normal.</p>

Table 1 (continued)

	DRUJ lies halfway between these. The center of rotation is then joined perpendicularly to the line depicting the length of the sigmoid notch.	
Congruency Method		
	Based on subjective evaluation of the arcs of the ulnar head and sigmoid notch.	Instability is present if the distance varies at any point.

volumes in axial plane can be played as a cine clip to assess the joint kinematics and evaluate the dynamic changes in the joint morphology, which provides a more functional idea of the pathology in its entirety (Fig. 7) [43]. The 4DCT imaging allows unconstrained joint motion and can potentially improve the pre-surgical planning with earlier detection of diseases (bone and tendon malalignments) before they progress to static lesions [44–46]. It can be done with weights but is typically performed without weights to avoid motion artifacts and misregistration on the reconstructed 3D volumes. It is, however, currently not known whether such a novel and advanced modality alters the patient outcomes.

### Magnetic resonance imaging

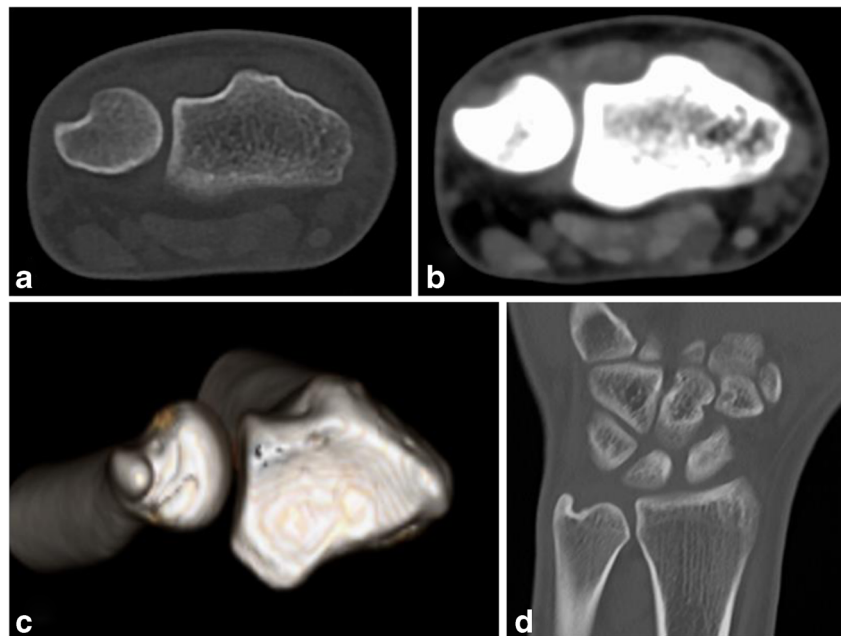
MRI remains the most sensitive modality for assessing soft tissue changes. It is essential that during wrist evaluation, appropriate sequences are chosen. A high spatial resolution (in-plane resolution of 0.3–0.5 mm) and high

signal-to-noise ratio intermediate-weighted imaging (non-fat-suppressed and fat-suppressed, echo time 35–45 ms, and matrix of 256 and above) is essential to properly evaluate these minute structures, attain good fluid–cartilage–ligament contrast-to-noise ratio, and avoid false diagnoses [47]. 3D images, especially with spin echo contrast and variable flip angle evolutions, can be obtained in isotropic sub 1-mm resolution in 6–7 min on a 3-Tesla scanner. These allow fine evaluation of these ligamentous structures and fibrocartilage of TFC. Sometimes these non-contrast MR exams are sufficient, but MR arthrography and traction have been advocated to detect subtle tears of ligaments and TFC in instability cases, such as in athletes [48]. MRI can also be obtained in static positionings of supination and pronation to detect bony instability (joint incongruity) apart from soft tissue evaluation using a wrist or small flex coil similar to the CT imaging.

The TFC proper, or articular disc, demonstrates biconcave low signal intensity on all sequences [49]. The ulnar



**Fig. 6** 3D and 4D CT (static frame reconstructed from real-time motion) images of the normal, congruent right DRUJ



attachment may appear hyperintense due to the presence of vascular, loose connective tissue between and around the upper and lower laminae [50, 51]. The axial view is optimal for visualization of the dorsal and volar radioulnar ligaments, the thickenings of the TFC at the dorsal and ulnar aspects (Fig. 8). The triangular ligament extends proximally from the ulnar styloid fovea to the ulnar styloid tip distally, and it is seen as a low-signal-intensity band attached to the fovea and styloid tip. It appears striated on coronal images and appears to have focal intermediate

signal intensity between the two attachments—the ligamentum subcruentum [4, 52] (Fig. 9). These variations in signal intensity should not be mistaken for tears. Tears show linear hyperintensity on T2-weighted images [52]. It is important to trace the dorsal and ulnar ligaments to their attachments to detect tears since the central disc may appear normal with these tears. Peripheral tears are more difficult to diagnose than central and are more often present with ulnar-sided wrist pain. These should be suspected if these radiologic signs are present: upper and/or lower

**Fig. 7** 4D (a and b) static frames reconstructed from real-time motion images and 3D reconstruction (c) demonstrate exact degree of dorsal ulnar subluxation in a patient with ulnar styloid fracture (arrow in d) and DRUJ instability

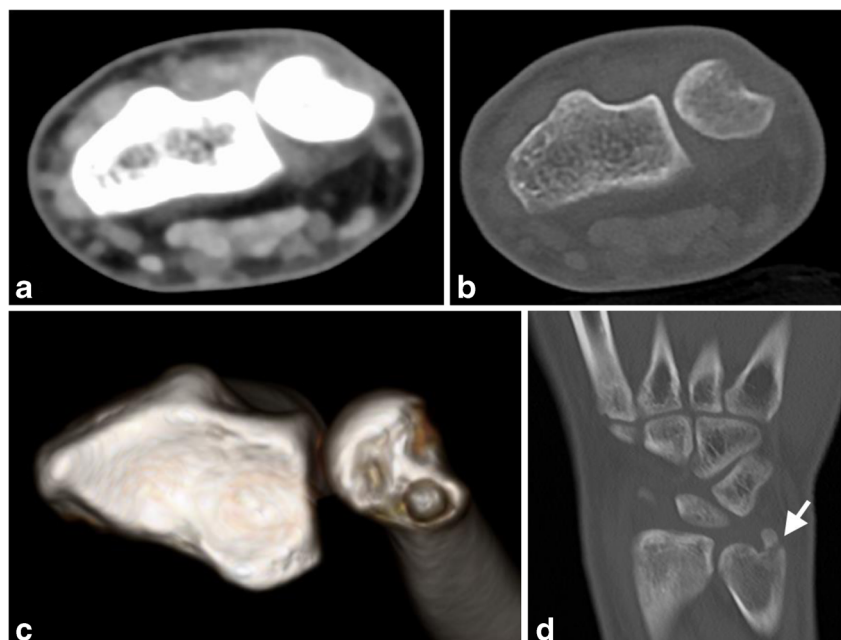
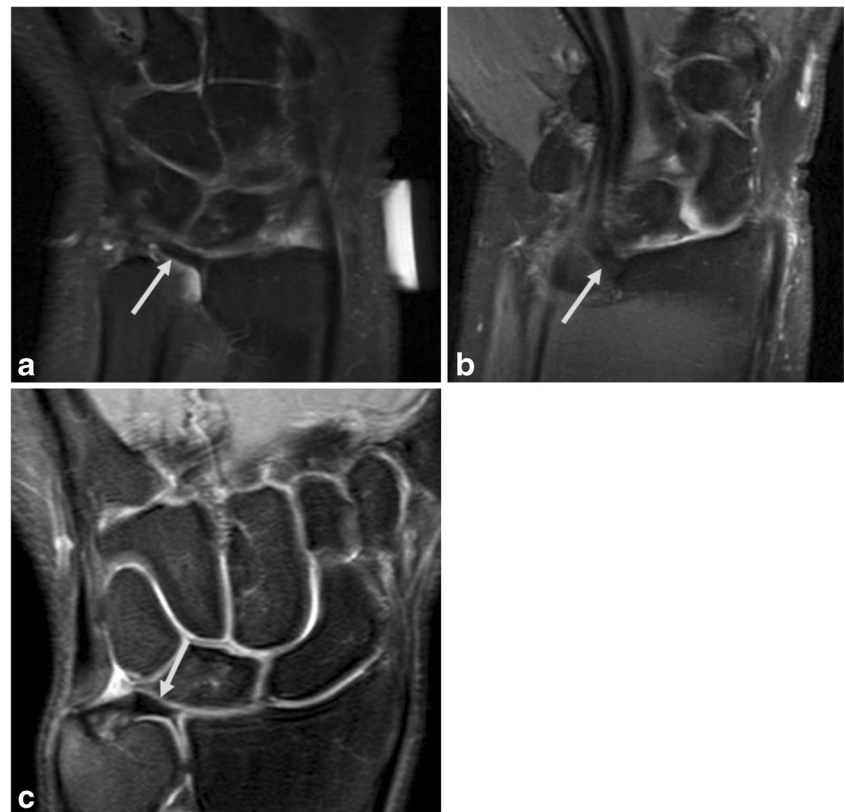


**Fig. 8** Pronated wrist MRI. Images obtained along the dorsal and volar aspects of the wrist demonstrate the normal hypointense and taut dorsal (arrow in **a**) and volar (arrow in **b**) radio-ulnar ligaments with bone-to-bone connection as opposed to TFCC (arrow in **c**) which connects the radial articular surface to the ulnar bony surface



lamina detachment from the ulna, high fluid signal intensity along the ulnar insertions, extension of fluid proximal to the base of ulnar styloid process, or focal adjacent synovitis, and it may warrant intravenous contrast or MR arthrography with injection [53]. It is also important to clinically correlate any pathology evident on imaging, as some findings may represent age-related degenerative changes that do not necessitate specific intervention. TFC degenerative changes show as increased signal intensity that does not extend to the articular surface. A central perforation in the TFCC in individuals over 50 years of age is a common finding [52, 54] (Fig. 10). The tears of dorsal and volar radioulnar ligaments are associated with volar

and dorsal radioulnar subluxation/dislocation, respectively. The ligament tears are evident as focal increased signal and/or discontinuity of the hypointense structure. The Palmer classification divides tears into traumatic and degenerative types (Table 2) [55]. The Atzei classification is a treatment-oriented classification based on clinical instability and arthroscopic findings (Table 3) (Fig. 1) [56].

Ulnar impaction syndrome is a chronic degenerative wrist condition, commonly seen in the middle-aged, caused by the chronic impaction of the head of the ulna against the carpals, predominantly the lunate. It is associated with a positive ulnar variance, usually due to developmental predisposition but may occur without

**Fig. 9** Post-MR arthrogram coronal fsT1 (**a**), fsPD (**b**), and sagittal fsT1 (**c**) images show mild increased signal of the ligamentum subcruciatum, a normal structure, and normal taut and continuous appearance of the ulnotriquetral ligament (large arrows)

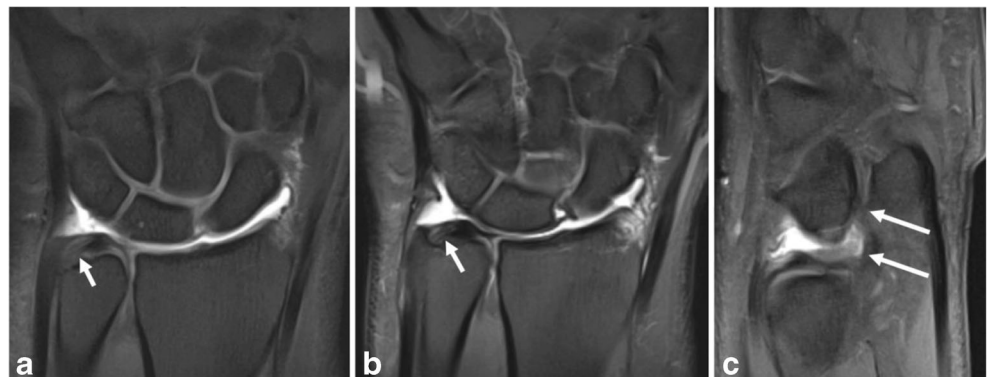
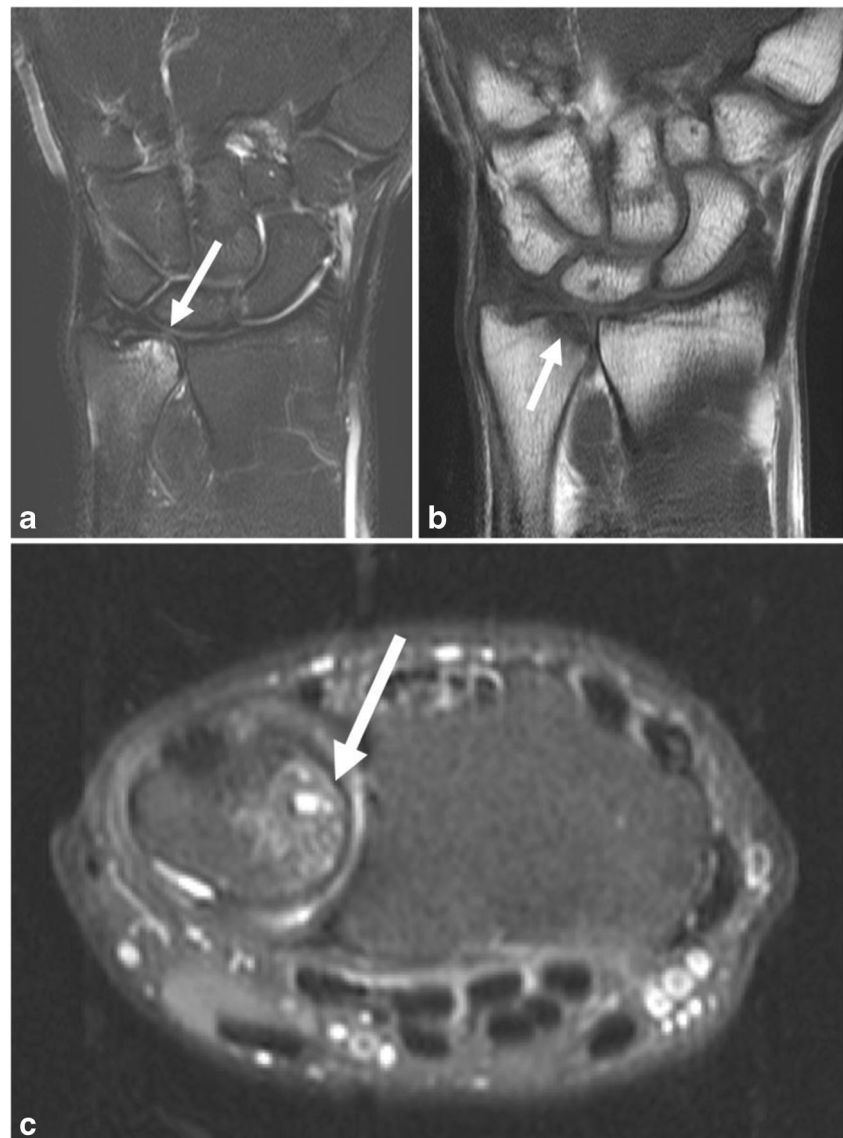


**Fig. 10** A 44-year-old male with TFCC perforation (*arrow*) on PD with fat-saturated image (**a**), and osteochondral lesion (*arrow*) of the ulnar head T1W coronal image (**b**) and axial PD with fat-saturated image (**c**)



predisposition if excessive repeated loading or strain is present, or in the setting of previous radial fracture and

**Table 2** Palmer's classification of complex TFC lesions

Classification	1 - Traumatic	2 - Degenerative
A	Central perforation	TFC wear
B	Ulnar avulsion	TFC wear and chondromalacia
C	Distal avulsion	TFC perforation and chondromalacia
D	Radial avulsion	TFC perforation, chondromalacia, and lunotriquetral ligament perforation
E		TFC perforation, chondromalacia, lunotriquetral ligament perforation, and ulnocarpal or radioulnar arthritis or both

shortening [57]. In chronic ulnocarpal abutment, the lunotriquetral ligament (LTL) can be affected along with degenerative tears of TFC and uncommonly, DRUJ articular lesions may be present (Fig. 10) (Table 1). The LTL has three components—linearly shaped volar band, triangular proximal component, and a dorsal band, which is the most important for maintaining carpal stability [58, 59]. Dorsal band tears may lead to volar intercalated carpal segmental instability. Detecting tears and abnormalities of this ligament can be challenging, however, disruption of proximal Gilula arc is a good indirect sign of its insufficiency. Thus, central tears of the triangular fibrocartilage, step-off between the lunate and triquetrum (disruption of Gilula A arc), and findings suggestive of ulnocarpal abutment are indications that warrant through assessment of LTL [60]. MRI is, in addition, invaluable for the evaluation of overlying cartilage [38]. Axial views in maximal

**Table 3** Atzei classification of TFCC peripheral tears

	Class 1 Repairable distal tear	Class 2 Repairable complete tear	Class 3 Repairable proximal tear	Class 4 Non- repairable tear	Class 5 Arthritic DRUJ
Clinical DRUJ instability	None/Slight	Mild/Severe	Mild/Severe	Severe	Mild/Severe
Status of TFCC distal component	Torn	Torn	Intact	Torn	Variable
Status of TFCC proximal component	Intact	Torn	Torn	Torn	
Healing potential of TFCC tear	Good	Good	Good	Poor	
Status of DRUJ cartilage	Good	Good	Good	Good	Poor
Treatment	Repair			Reconstruction	Salvage

pronation and supination have been found to be useful in detecting chondral degeneration. It is important to remember that the ulnar volar facet is normally devoid of cartilage.

MRI is also excellent for bone marrow evaluation and finding synovitis (Fig. 11). Synovitis is best detected on intravenous contrast administration and is an indicator of various pathologies including tears of a surrounding ligament or tendon, arthritis, and Keinboch's disease. The prestyloid recess is a synovium-lined pouch that is directly connected to the radiocarpal compartment and is surrounded by meniscal homologue distally, the TFCC attachment to ulnar styloid proximally and central TFCC disk radially. It may vary in shape, i.e., saccular (38%), tubular (18%), and conical or tongue-shaped (13%) [52], and it is important to not confuse normal anatomical variants with pathology. Synovial osteochondromatosis of the DRUJ is a disorder of unknown etiology characterized by metaplasia of the subsynovial cells resulting in hyperplasia and the formation of cartilaginous or osseocartilaginous nodules shed as loose bodies into the synovial cavity. It may be a primary or secondary disorder. It is commonly seen in the 2nd to 4th decades and is more common in men, who present with complaints of gradually progressive pain, swelling, locking, and limited range of motion. On MR, it is seen to have chondroid signal characters and has

intermediate to low signal on T1 and high signal on T2 (Fig. 12). While usually benign and more common in larger joints, it is an important diagnosis to consider due to the risk of malignant transformation, and as a differential of other pathologies of the wrist, such as rheumatoid arthritis (RA), OA, chondrocalcinosis, synovial chondrosarcoma, etc. [61]. RA pannus typically erodes the base of the ulnar styloid process and can secondarily lead to ulnar shortening and painful impingement on distal radius metaphysis (Fig. 13).

Standard MRI has been found to be highly specific, but not sensitive for detecting tears of the intrinsic ligament as compared to the gold standard of arthroscopy. Direct MR arthrography, with contrast material injected into the joint, can be especially useful for evaluating the TFCC and other wrist ligaments facilitated by superior contrast resolution, joint distension and flow of contrast in different wrist compartments (Figs. 14, 15, 16). It is useful in distinguishing between the presence of a tear, as indicated by the presence of both fluid and contrast in the DRUJ, or other mechanical or inflammatory fluid, which would be devoid of gadolinium. There is no consensus on guidelines, but usually, a radiocarpal injection is done in most cases. Rarely, if no defects are visualized but suspicion remains high, a DRUJ injection may be supplemented

**Fig. 11** Wrist synovitis; 35-year-old man with wrist pain. PA radiographs were reported as normal. Coronal fsPD image shows bone marrow edema of proximal radial-sided carpus with trace fluid in the joint. Perfusion MR image shows active synovitis on the radial side of the wrist. The serology was subsequently positive for rheumatoid arthritis

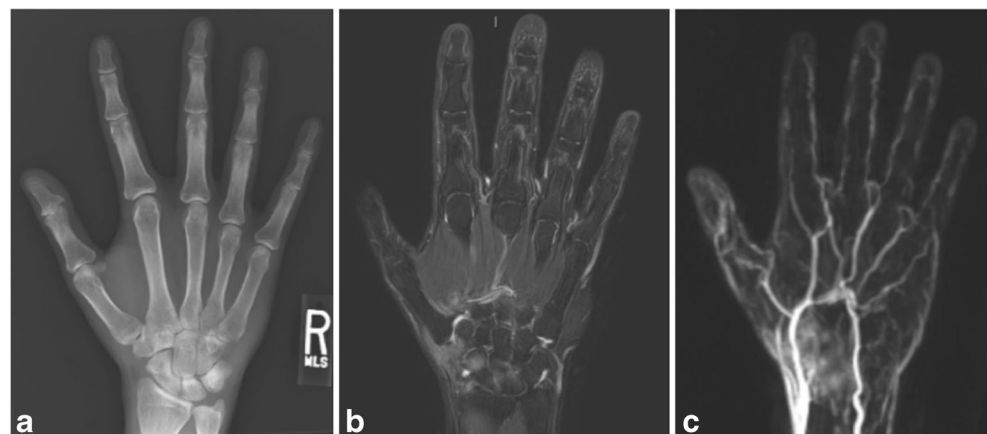
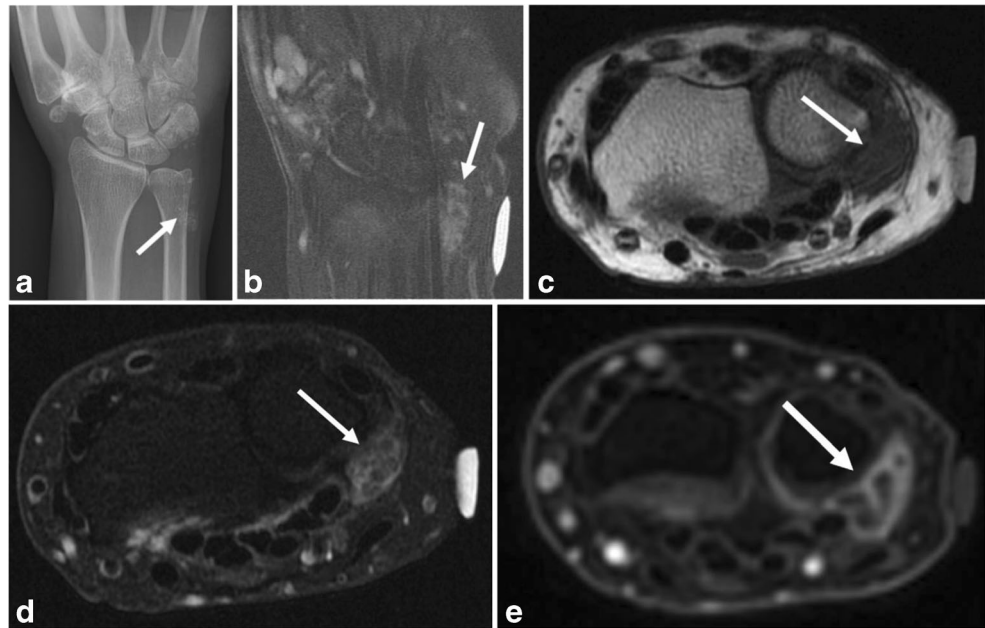


**Fig. 12** A 50-year-old woman with primary synovial osteochondromatosis seen on PA radiographs (**a**), showing multiple small calcified foci (*arrow*) along the medial aspect of the ulna. STIR coronal (**b**), T1W axial (**c**), PD with fat-saturated axial (**d**), and axial post-contrast T1W (**e**) images demonstrate hypointense foci (*arrow* in **b**, **c**, **d**) surrounded by peripheral enhancement (*arrow* in **e**)



[62]. Direct MRA remains limited by its invasiveness and increased cost. The utility of indirect MR arthrography using IV contrast that perfuses gradually into the joint, is debated. The dependence of contrast on perfusion and vascularity poses a problem due to the effect on signal intensity that may make it difficult to detect disease [6].

3D imaging and kinematic MR imaging are still being explored in the domains of DRUJ instability and wrist

pathology. Volumetric isotropic imaging allows ligament evaluation in high resolution with images reconstructed in the planes of DRUJ and radioulnar ligaments [63, 64]. Kinematic imaging with real-time unconstrained motion and acquisition of imaging in axial planes with real-time manipulation of imaging planes like cardiac imaging is possible. However, the clinical value of such imaging and its impact on patient management is not yet known.



**Fig. 13** PA radiograph demonstrates secondary OA superimposed on RA of DRUJ (*arrow*) with eroded ulnar styloid process and ulnar translocation of the carpus

## Treatment

Conservative treatment is always attempted initially in chronic or subacute DRUJ dysfunction and involves reduction or modification of activity, occupational and physical therapy, splinting, and the use of NSAIDs or intraarticular steroid injections [23]. In case of instability due to fracture/subluxation, reduction is needed to ensure integrity of the joint anatomy to allow for soft tissue healing. In distal radius fractures, reduction and restoration of radial alignment is necessary and long-term results show no differences in the outcomes of conservative versus surgical approaches [65]. Ulnar head dislocations may require reduction and temporary fixation with K-wires. For fracture of the ulnar styloid, fixation of the radius alone may have the same results as ulnar styloid fixation [66]. While most commonly soft tissue injuries heal after bone reduction, instability may persist in some cases, especially in younger patients. In these cases, it is essential to evaluate after 4–6 weeks, and treat possible TFCC tears or consider styloid fixation [23]. Surgical repair, either

**Fig. 14** A 54-year-old female with pain and DRUJ instability. Coronal fsPD (a) and post MR arthrogram fsT1W (b) images show the completely tom upper lamina of TFC disc (*large arrow*) and partially tom lower lamina (styloid attachment, *small arrow*). Sagittal fsT1W image (c) shows frayed ulnotriquetral ligament (*arrow*). Axial fsT1W image shows the irregular and thickened volar RU ligament (*small arrow*) with mild dorsal subluxation of the ulna (d). Notice leakage of contrast from the ligament and adjacent capsule (*large arrow*)

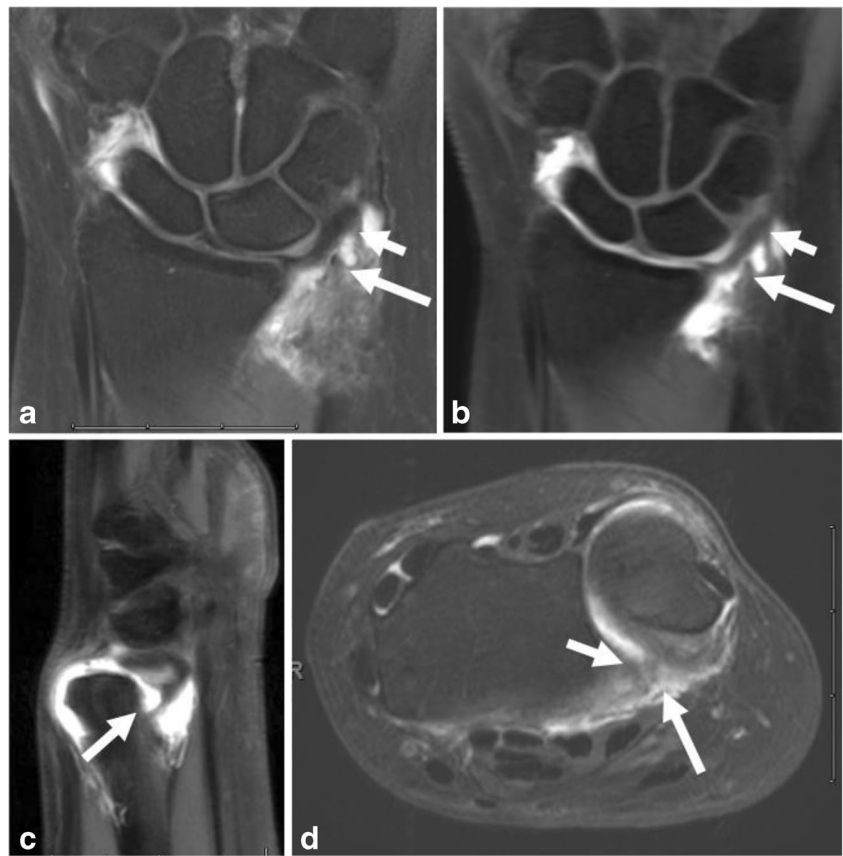


**Fig. 15** A 66-year-old female with wrist pain. Post-MR arthrogram coronal fsT1W (a, b) and sagittal fsT1W (c) images show the completely tom ulnotriquetral ligament (*small arrow* in a, c) and lower lamina of TFC disc (*small arrow* in b). Coronal 3D PDW image shows the intact upper lamina of the TFC (*large arrow*) (d)

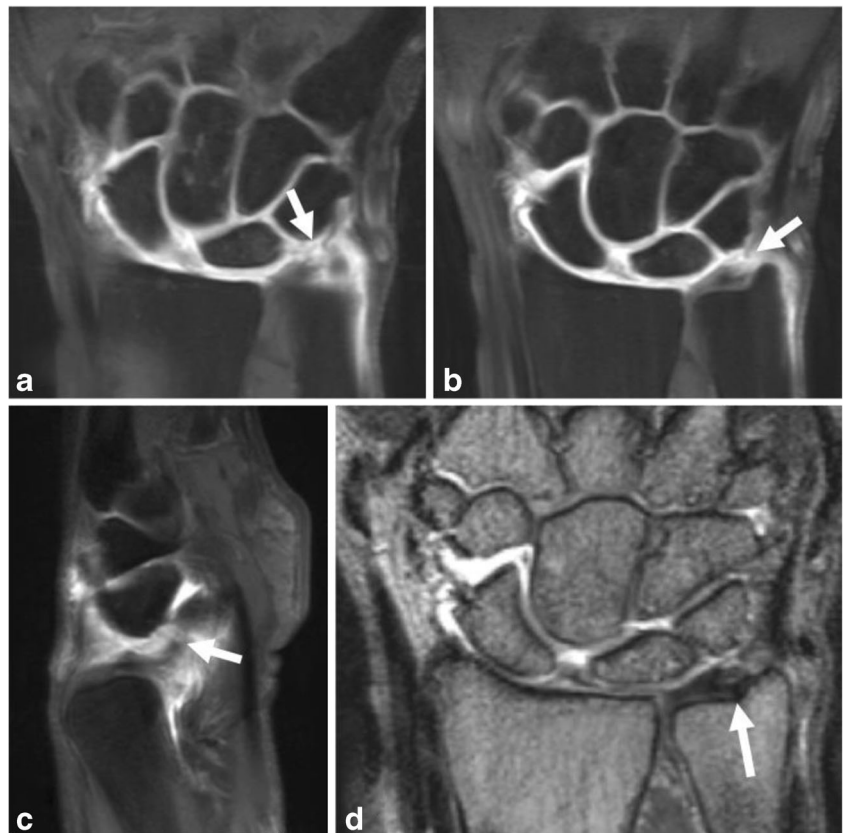
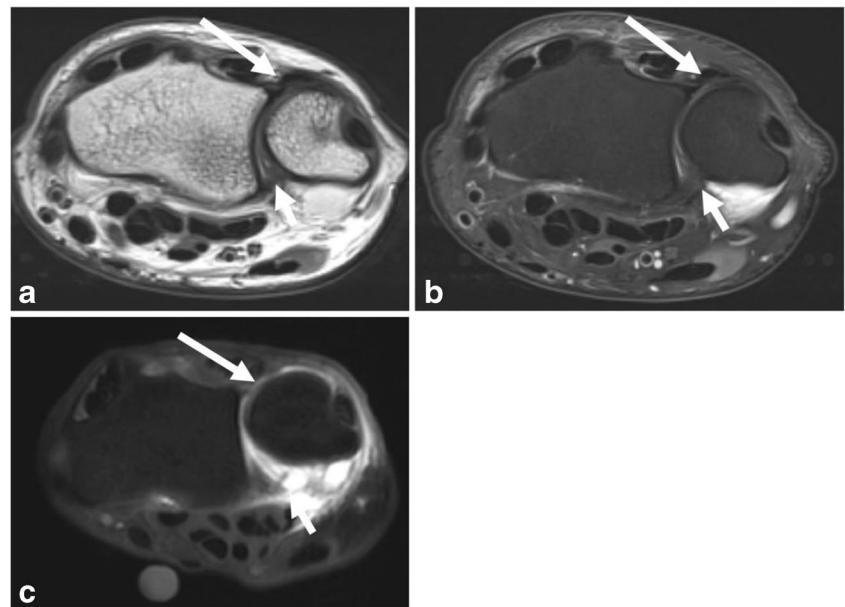


**Fig. 16** Normal and abnormal DRUJ ligament. **a, b** Axial PD and fsT1 images from a MR arthrogram show normal DRUJ alignment and normal volar (*small arrow*) and dorsal DRUJ (*large arrow*) ligaments. **c** Axial fsT1W image from a patient with DRUJ instability and pain showing tear of the volar DRUJ ligament (*small arrow*) with contrast extravasation. Notice intact dorsal DRUJ ligament and mild dorsal subluxation of the ulna (*large arrow*)



arthroscopic or open, is considered once conservative management has failed.

Open repair is especially considered in unstable DRUJ injuries and 6–8 weeks of continued symptoms due to foveal disruption of TFCC, chronic arthritis (Fig. 13), or non-arthritic instability. There are three broad surgical

options that may be considered: resection arthroplasty, implant arthroplasty, or salvage procedures as a last resort. The Darrach procedure (Fig. 17) is a form of resection arthroplasty that involves removal of the distal ulna. It is usually indicated to provide pain relief caused by distal RU disruption or severe RU arthritis. It has been shown

**Fig. 17** Darrach procedure. Distal ulnar osteotomy (*arrow* in **a** and **b**) on CT images of DRUJ. Fat-saturated T2W coronal (**c**) and axial (**d**) images demonstrate susceptibility artifacts and bone marrow edema related to surgery (*arrows*). Notice chronic remodeling/erosion of the distal radius at the DRUJ with smooth cortical scalloping due to the long standing ulnar impingement

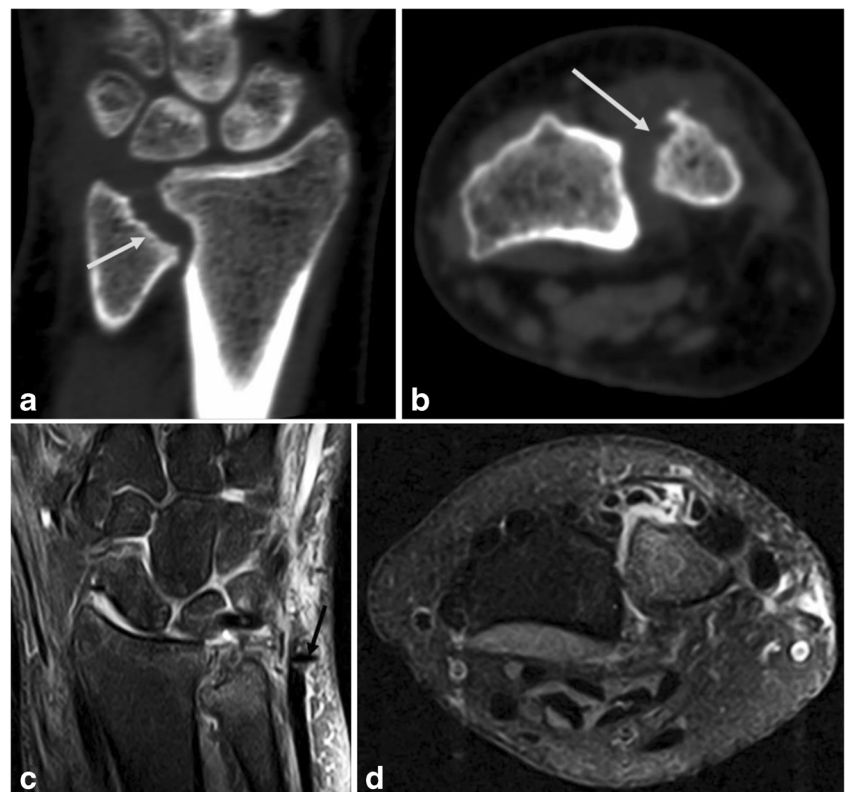
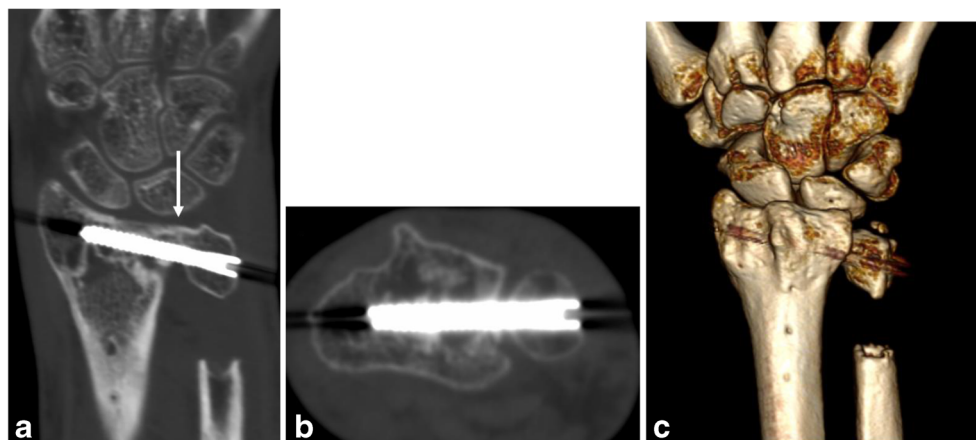


**Fig. 18** Sauvé–Kapandji procedure. Coronal (a), axial (b), and 3D (c) CT images demonstrate partial osteotomy of distal ulna with preservation of the ulnar head and partial fusion of the DRUJ (arrow in a)



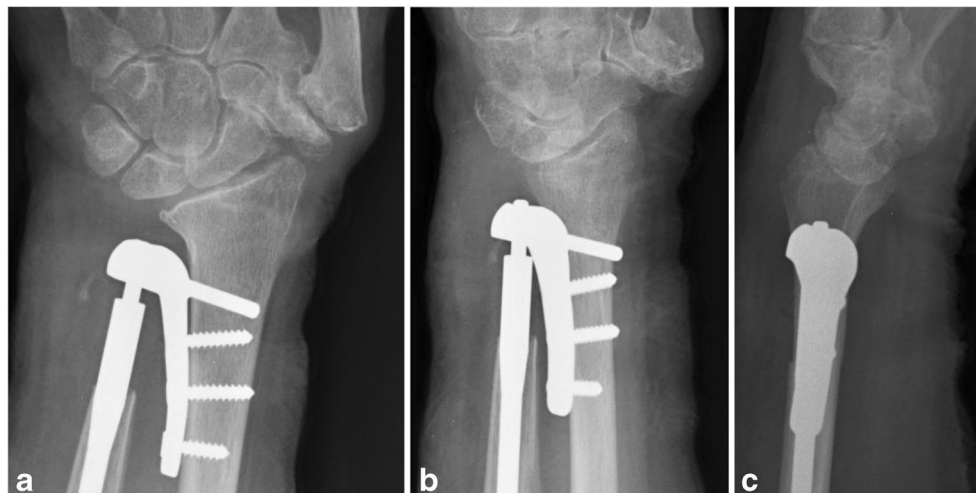
to improve pronation and supination. Its limitations include: possible developments of ulna impingement syndrome, decreased grip strength, and ulnar translation of carpals [67, 68]. Since it leaves the patient with low functionality, it is preferred for the elderly. It may also be combined with ECU or FCU tendon slings to provide more ulnar support [14, 69]. Various hemiresection procedures with interposition of soft tissues between the remaining ulnar stump and radius are other options. A more function-preserving choice is the Sauvé–Kapandji procedure (Fig. 18) that involves arthrodesis of DRUJ, which is more commonly preferred in young patients. Forearm pronation and supination are maintained by creating a pseudoarthrosis of the ulna just proximal to the DRUJ arthrodesis. It differs from the Darrach procedure in that it preserves ulnar support of the wrist, as the distal radioulnar ligaments and ulnocarpal ligaments are maintained but painful instability of the proximal ulna stump may persist [14, 68]. Various implants like partial or total ulnar head replacement, or a total DRUJ arthroplasty

(Fig. 19), are other options. Salvage procedures may often sacrifice the range of motion in favor of pain relief and preservation of some function and strength. Options of such an approach include: creation of a one-bone forearm, wide excision of the distal ulna, or the three-component reconstruction Kleinman–Greenberg procedure, which may be done to salvage and stabilize a previously failed Darrach procedure [70].

## Conclusions

DRUJ dysfunction, instability, and/or pain is an important problem that frequently necessitates patient evaluation using radiography and advanced imaging methods since clinical examination provides only subtle clues towards the final diagnosis. Knowledge of the complex anatomy of the DRUJ and adjacent structures is essential for the proper interpretation of imaging studies to allow accurate diagnosis and treatment.

**Fig. 19** DRUJ replacement. PA (a), oblique (b), and sagittal (c) radiographs show DRUJ replacement using Scheker prosthesis (Aptis Medical, Glenview, KY)





**Acknowledgements** The authors acknowledge Ms. Erin Moore and Mr. Jon Garinn for their contribution to the illustrations.

## Compliance with ethical standards

**Disclosures** AC: Consultant ICON Medical, Royalties: Jaypee, Wolters.

**Conflict of interest** None.

## References

- Lees V. Functional anatomy of the distal radioulnar joint in health and disease. *Ann R Coll Surg Engl*. 2013;95(3):163–70.
- Garrigues GE, Sabesan V, Aldridge JM III. Acute distal radioulnar joint instability. *J Surg Orthop Adv*. 2008;17(1548–825X (Print)):262–6.
- Wassink S, Lisowski LA, Schutte BG. Traumatic recurrent distal radioulnar joint dislocation: a case report. *Strateg Trauma Limb Reconstr*. 2009;4(3):141–3.
- Squires JH, England E, Mehta K, Wissman RD. The role of imaging in diagnosing diseases of the distal radioulnar joint, triangular fibrocartilage complex, and distal ulna. *Am J Roentgenol*. 2014;203:146–53.
- Wijffels M, Brink P, Schipper I. Clinical and non-clinical aspects of distal radioulnar joint instability. *Open Orthop J*. 2012;6:204–10.
- Watanabe A, Souza F, Vezeridis PS, Blazar P, Yoshioka H. Ulnar-sided wrist pain. II. Clinical imaging and treatment. *Skelet Radiol*. 2010;39:837–57.
- Szabo RM. Distal radioulnar joint instability. *Instr Course Lect*. 2007;56:79–89.
- Tolat AR, Stanley JK, Trail IA. A cadaveric study of the anatomy and stability of the distal radioulnar joint in the coronal and transverse planes. *J Hand Surg Eur Vol*. 1996;21(5):587–94.
- Wolfe SW, Hotchkiss RN, Pederson WC, Kozin SH, Cohen MS. Revision of: Green DP. Green's operative hand surgery. Vol. 2, Green's Operative Hand Surgery. 2011. 1775–2005 p.
- Ekenstam FA, Hagert CG. Anatomical studies on the geometry and stability of the distal radio ulnar joint. *Scand J Plast Reconstr Surg*. 1985;19(1):17–25.
- Pirela-Cruz MA, Goll SR, Klug M, Windler D. Stress computed tomography analysis of the distal radioulnar joint: a diagnostic tool for determining translational motion. *J Hand Surg Am*. 1991;16(1):75–82.
- Mespreuve M, Vanhoenacker F, Verstraete K. Imaging findings of the distal radio-ulnar joint in trauma. *J Belgian Soc Radiol*. 2015;99(1):1–20.
- Palmer AK, Werner FW. The triangular fibrocartilage complex of the wrist—anatomy and function. *J Hand Surg Am*. 1981;6(2):153–62.
- Thomas BP, Sreekanth R. Distal radioulnar joint injuries. *Indian J Orthop*. 2012;46(5):493–504.
- Palmer AK, Werner FW. Biomechanics of the distal radioulnar joint. *Clin Orthop Relat Res*. 1984;26–35.
- Kouwenhoven STP, De Jong T, Koch AR. Dorsal capsuloplasty for dorsal instability of the distal ulna. *J Wrist Surg*. 2013;2(2):68th Annual Meeting of the ASSH: Education through.
- Omokawa S, Tanaka Y, Fujitani R. Radiographic predictors of DRUJ instability with distal radius fractures. *J Wrist Surg*. 2014;3(1):2–6.
- Hagert CG. Distal radius fracture and the distal radioulnar joint—anatomical considerations. *Handchir Mikrochir Plast Chir*. 1994;26(1):22–6.
- Skalski MR, White EA, Patel DB, Schein AJ, RiveraMelo H, Matcuk GR. The traumatized TFCC: an illustrated review of the anatomy and injury patterns of the triangular fibrocartilage complex. *Curr Probl Diagn Radiol*. 2016;45(1):39–50.
- Matthias R, Wright TW. Interosseous membrane of the forearm. *J Wrist Surg*. 2016;5(3):188–93.
- Hutchinson S, Faber KJ, Gan BS. The Essex–Lopresti injury: more than just a pain in the wrist. *Can J Plast Surg*. 2006;14(4):215–8.
- Coggins CA. Imaging of ulnar-sided wrist pain. *Clin Sports Med*. 2006;25(3):505–26.
- Baek GH, Kato H, Romanowski L. IFSSH Scientific Committee on Bone and Joint Injuries: Distal Radioulnar Joint Instability. 2012; (November). [http://www.ifssh.info/2012\\_Bone\\_and\\_Joint\\_Injuries\\_Distal\\_Radioulnar\\_Joint\\_Instability.pdf](http://www.ifssh.info/2012_Bone_and_Joint_Injuries_Distal_Radioulnar_Joint_Instability.pdf).
- Andersson JK, Lindau T, Karlsson J, Fridén J. Distal radio-ulnar joint instability in children and adolescents after wrist trauma. *J Hand Surg Eur Vol*. 2014;39(6):653–61.
- Fornalski S, Lee TQ, Gupta R. Chronic instability of the distal radioulnar joint: a review. *Univ Pennsylvania Orthop J*. 2000;13:43–52.
- Lester B, Halbrecht J, Levy IM, Gaudinez R. “Press test” for office diagnosis of triangular fibrocartilage complex tears of the wrist. *Ann Plast Surg*. 1995;3:41–5.
- Ng CY, Hayton MJ. Ice cream scoop test: a novel clinical test to diagnose extensor carpi ulnaris instability. *J Hand Surg Eur Vol*. 2013;38:569–70.
- Tsai PC, Paksima N. The distal radioulnar joint. *Bull NYU Hosp Jt Dis*. 2009;67(1):90–6.
- Loredo RA, Sorge DG, Garcia G. Radiographic evaluation of the wrist: a vanishing art. *Semin Roentgenol*. 2005;40:248–89.
- Palmer AK. The distal radioulnar joint. Anatomy, biomechanics, and triangular fibrocartilage complex abnormalities. *Hand Clin*. 1987;3(1):31–40.
- Mino DE, Palmer AK, Levinsohn EM. The role of radiography and computerized tomography in the diagnosis of subluxation and dislocation of the distal radioulnar joint. *J Hand Surg Am*. 1983;8(1):23–31.
- Yang Z, Mann FA, Gilula LA, Haerr C, Larsen CF. Scaphoiscapitate alignment: criterion to establish a neutral lateral view of the wrist. *Radiology*. 1997;205(3):865–9.
- Nakamura R, Horii E, Imaeda T, Tsunoda K, Nakao E. Distal radioulnar joint subluxation and dislocation diagnosed by standard roentgenography. *Skelet Radiol*. 1995;24(2):91–4.
- Hess F, Farshad M, Sutter R, Nagy L, Schweizer A. A novel technique for detecting instability of the distal radioulnar joint in complete triangular fibrocartilage complex lesions. *J Wrist Surg*. 2012;1(2):153–8.
- Duryea DM, Payatakes AH, Mosher TJ. Subtle radiographic findings of acute, isolated distal radioulnar joint dislocation. *Skelet Radiol*. 2016;45(9):1243–7.
- Ehman EC, Felmlee JP, Frick MA. Imaging of the proximal and distal radioulnar joints. *Magn Reson Imaging Clin N Am*. 2015;23:417–25.
- Wijffels M, Stomp W, Krijnen P, Reijnierse M, Schipper I. Computed tomography for the detection of distal radioulnar joint instability: normal variation and reliability of four CT scoring systems in 46 patients. *Skelet Radiol*. 2016;45(11):1487–93.
- Chiang C-C, Chang M-C, Lin CFJ, Liu Y, Lo W-H. Computerized tomography in the diagnosis of subluxation of the distal radioulnar joint. *Chin Med J*. 1998;61(12):708–15.
- Dumonteil S, Shah MA, Srikanthan A, Ejindu V, Papadakos N. ESSR 2016 / P-0114 Dynamic CT Assessment of Distal Radioulnar Instability. 2016. <https://doi.org/10.1594/essr2016/P-0114>.

40. Wechsler RJ, Wehbe MA, Rifkin MD, Edeiken J, Branch HM. Computed tomography diagnosis of distal radioulnar subluxation. *Skelet Radiol*. 1987;16(1):1–5.
41. Park MJ, Kim JP. Reliability and normal values of various computed tomography methods for quantifying distal radioulnar joint translation. *J Bone Joint Surg Am*. 2008;90(1):145–53.
42. Kalia V, Obray RW, Filice R, Fayad LM, Murphy K, Carrino JA. Functional joint imaging using 256-MDCT: Technical feasibility. *Am J Roentgenol*. 2009;192(6):W295.
43. Demehri S, Hafezi-Nejad N, Morelli JN, Thakur U, Lifchez SD, Means KR, et al. Scapholunate kinematics of asymptomatic wrists in comparison with symptomatic contralateral wrists using four-dimensional CT examinations: initial clinical experience. *Skelet Radiol*. 2016;45(4):437–46.
44. Kakar S, Breighner R, Leng S, McCollough C, Moran S, Berger R, et al. The role of dynamic (4D) CT in the detection of scapholunate ligament injury. *J Wrist Surg*. 2016;05(04):306–10.
45. Leng S, Zhao K, Qu M, An K-N, Berger R, McCollough CH. Dynamic CT technique for assessment of wrist joint instabilities. *Med Phys*. 2011;38(S1):S50–6.
46. Shores JT, Demehri S, Chhabra A. Kinematic “4 dimensional” CT imaging in the assessment of wrist biomechanics before and after surgical repair. *Eplasty*. 2013;13:e9.
47. Srivastava D, Sharma R, Gamanagatti S, Kotwal P, Sharma V, Pahwa S. Comparison of conventional MRI and MR arthrography in the evaluation wrist ligament tears: a preliminary experience. *Indian J Radiol Imaging*. 2014;24(3):259.
48. Ng AWH, Griffith JF, Fung CSY, Lee RKL, Tong CSL, Wong CWY, et al. MR imaging of the traumatic triangular fibrocartilaginous complex tear. *Quant Imaging Med Surg*. 2017;7(4):443–60.
49. Vezeridis PS, Yoshioka H, Han R, Blazar P. Ulnar-sided wrist pain. Part I: anatomy and physical examination. *Skelet Radiol*. 2010;39:733–45.
50. Sugimoto H, Shinozaki T, Ohsawa T. Triangular fibrocartilage in asymptomatic subjects: investigation of abnormal MR signal intensity. *Radiology*. 1994;191(1):193–7.
51. Nakamura T, Takayama S, Horiuchi Y, Yabe Y. Origins and insertions of the triangular fibrocartilage complex: a histological study. *J Hand Surg Am*. 2001;26(5):446–54.
52. Burns JE, Tanaka T, Ueno T, Nakamura T, Yoshioka H. Pitfalls that may mimic injuries of the triangular fibrocartilage and proximal intrinsic wrist ligaments at MR imaging. *Radiographics*. 2011;31:63–78.
53. Rüegger C, Schmid MR, Pfirrmann CWA, Nagy L, Gilula LA, Zanetti M. Peripheral tear of the triangular fibrocartilage: depiction with MR arthrography of the distal radioulnar joint. *Am J Roentgenol*. 2007;188(1):187–92.
54. Mikić ZD. Age changes in the triangular fibrocartilage of the wrist joint. *J Anat*. 1978;126:367–84.
55. Palmer AK. Triangular fibrocartilage complex lesions: a classification. *J Hand Surg Am*. 1989;14(4):594–606.
56. Atzei A. New trends in arthroscopic management of type 1-B TFCC injuries with DRUJ instability. *J Hand Surg Eur Vol*. 2009;34(5):582–91.
57. Tomaino MM. Ulnar impaction syndrome in the ulnar negative and neutral wrist. Diagnosis and pathoanatomy. *J Hand Surg Br*. 1998;23(6):754–7.
58. Yoshioka H, Tanaka T, Ueno T, Shindo M, Carrino JA, Lang P, et al. High-resolution MR imaging of the proximal zone of the lunotriquetral ligament with a microscopy coil. *Skelet Radiol*. 2006;35:288–94.
59. Bateni CP, Bartolotta RJ, Richardson ML, Mulcahy H, Allan CH. Imaging key wrist ligaments: what the surgeon needs the radiologist to know. *Am J Roentgenol*. 2013;200:1089–95.
60. Ringler MD. MRI of wrist ligaments. *J Hand Surg Am*. 2013;38(10):2034–46.
61. McInnes CW, Goetz TJ. Management of synovial osteochondromatosis of the distal radioulnar joint with imaging features consistent with malignancy. *Case Rep Orthop*. 2013;2013:589631.
62. Maizlin ZV, Brown JA, Clement JJ, Grebenyuk J, Fenton DM, Smith DE, et al. MR arthrography of the wrist: controversies and concepts. *Hand*. 2009;4(1):66–73.
63. Sutherland JK, Nozaki T, Kaneko Y, Yu HJ, Rafijah G, Hitt D, et al. Initial experience with 3D isotropic high-resolution 3 T MR arthrography of the wrist. *BMC Musculoskelet Disord*. 2016;17(1):30.
64. Nozaki T, Der Wu W, Kaneko Y, Rafijah G, Yang L, Hitt D, et al. High-resolution MRI of the ulnar and radial collateral ligaments of the wrist. *Acta Radiol*. 2017;58(12):1493–9.
65. Lee SK, Kim KJ, Cha YH, Choy WS. Conservative treatment is sufficient for acute distal radioulnar joint instability with distal radius fracture. *Ann Plast Surg*. 2016;77(3):297–304.
66. Kim JK, Koh Y-D, Do N-H. Should an ulnar styloid fracture be fixed following volar plate fixation of a distal radial fracture? *J Bone Joint Surg Am*. 2010;92(1):1–6.
67. Kirk Watson H, Brown RE. Ulnar impingement syndrome after Darrach procedure: treatment by advancement lengthening osteotomy of the ulna. *J Hand Surg Am*. 1989;14(2 PART 1):302–6.
68. Lluch A. The Sauvé-Kapandji procedure: indications and tips for surgical success. *Hand Clin*. 2010;26:559–72.
69. Breen TF, Jupiter JB. Extensor carpi ulnaris and flexor carpi ulnaris tenodesis of the unstable distal ulna. *J Hand Surg Am*. 1989;14(4):612–7.
70. Kleinman WB, Greenberg JA. Salvage of the failed Darrach procedure. *J Hand Surg Am*. 1995;20(6):951–8.